Dalton Transactions

Accepted Manuscript

ROYAL SOCIETY OF CHEMISTRY

www.rsc.org/dalton

Journal Name

RSCPublishing

ARTICLE

Polyoxometalate-based organic-inorganic hybrid compounds containing transition metal mixed-organic-ligand complexes of N-containing and pyridinecarboxylate ligands

De-Chuan Zhao,[a] Yang-Yang Hu,[a] Hong Ding,[a] Hai-Yang Guo,[a] Xiao-Bing Cui[a]* Xiao Zhang,[b]* Qi-Sheng Huo[a] and Ji-Qing Xu[a]

research Cite this: DOI: 10.1039/x0xx00000x

Received 00th January 2012,
Accepted 00th January 2012

DOI: 10.1039/x0xx00000x

www.rsc.org/

Five new organic-inorganic hybrid compounds based on the Keggin-type polyoxoanion $[SiW_{12}O_{40}]^{4-}$, namely $[Cu_3(2,2'\text{-bpy})_3(inic)(\mu_2\text{-}OH)(H_2O)][SiW_{12}O_{40}]\cdot 2H_2O$ (**1**), $[Cu_6(phen)_6(\mu_3\text{-}Cl)_2(\mu_2\text{-}Cl)_2Cl_2(inic)_2][SiW_{12}O_{40}]\cdot 6H_2O$ (**2**), $[Cu_2(hnic)(2,2'\text{-bpy})_2Cl]_2[H_2SiW_{12}O_{40}]$ (**3**), $[Cu_2(nic)(phen)_2Cl_2]_2[SiW_{12}O_{40}]$ (**4**) and $[Cu_2(pic)(2,2'\text{-bpy})_2Cl]_2[SiW_{12}O_{40}]$ (**5**) (inic = isonicotinic acid, hnic = 2-hydroxy-nicotinic acid, nic =nicotinic acid, pic = picolinic acid, 2,2'-bpy=2,2'-bipyridine, phen=1,10-phenanthroline) have been synthesized and characterized by IR, UV-Vis, XPS spectrum, XRD, cyclic voltammetric measurements, photoluminescence analysis and single crystal X-ray diffraction analysis. Crystal analysis reveals that compound **1** exhibits a 2-D double layer framework structure constructed from $[SiW_{12}O_{40}]^{4-}$ and copper-aqua-2,2'-bipy-hydroxyl-isonicotinate complexes. Compound **2** is a 0-D discrete structure formed by $[SiW_{12}O_{40}]^{4-}$ and copper-chloro-isonicotinate-phenanthroline complexes. Compound **3** shows a 1-D single chain structure based on the linkage of copper-2,2-bpy-chloro-2-hydroxy-nicotinate complexes and $[SiW_{12}O_{40}]^{4-}$. Compounds **4** and **5** both contain polyoxometalate supported transition metal complexes, one is a polyoxometalate supported copper-chloro-nicotinate-phenanthroline complex in **4**, and the other is a polyoxometalate supported copper-2,2-bpy-chloro-nicotinate complex in **5**. It should be noted that the nicotinic, isonicotinic and picolinic acid are structural isomers and the 2-hydroxy-nicotinic acid is an in-situ hydroxylated product of the nicotinic acid. In addition, photocatalytic degradations of Rhodamine B (RhB) by compounds **1**-**5** have been investigated in aqueous solutions.

Introduction

Polyoxometalates (POMs) form a distinctive class of inorganic metal-oxygen cluster compounds which is unique in its topological and electronic versatility and useful in fields as diverse as catalysis, analysis, biochemistry, material science and medicine.[1] The class of POMs has been known for almost 200 years, but the first structural details were only revealed in the last century.[2] Up to now, POM chemistry continues to be a considerable focus in the ongoing research because of large numbers of POM structures and their properties. Many of fundamental properties of POMs that impact their applications, including elemental composition, solubility, redox potential(s), charge density, size, and shape, can be systematically altered to a considerable degree.[3]

Current research interests are mainly driven by the combination of POMs and N-containing organic moieties or transition metal N-containing organic complexes into POM-based hybrids.[4] Our group has focused on preparations, structures and properties of hybrids constructed from POMs and transition metal N-containing organic complexes for several years.[5] Based on an analysis of the literatures hitherto reported, [4,5] we find that each transition metal complex (TMC) of such POM-based organic-inorganic hybrids is almost always comprised of a metal ion and a type of organic ligands. That is to say, hybrids formed by POMs and transition metal mixed-organic-ligand complexes (TMMCs) are pretty rare. It is worthy to note that the direct introduction of N-containing organic moieties or transition metal N-containing complexes into POM compounds can not only enrich POM structures, but also ameliorate their polar, electricity, acid, and redox properties. [6] The introduction of TMMCs thereby may give rise to compounds with more interesting structures, topologies, and properties.

According to different TMMC organic ligands, the POM-based hybrids containing TMMCs could be divided into three types: namely type **1**, type **2** and type **3**. Type **1** hybrids contain more than one type of TMMC N-containing organic ligands;[7] type **2** hybrids contain more than one type of TMMC carboxylates; type **3** hybrids contain more than one type of TMMC organic ligands being composed of both N-containing organic ones and carboxylates.[8,9] To our knowledge, several type **1** hybrids were synthesized;[7] still no type **2** hybrids have been reported; type **3** compounds have been only rarely reported,[8,9] and carboxylate ligands in these type **3** compounds are the simplest aliphatic dicarboxylate, namely oxalate acid[8] and the pyridinecarboxylate, namely isonicotinic acid.[9]

We have recently synthesized some type **1** hybrids, [10] and then we want to further our synthesis to type **2** and type **3** hybrids, each of which contains carboxylates. It should be noted that carboxylate ligands are widely used in the formations of many materials especially MOFs.[11] However, the introduction of carboxylates into POM compounds has remained largely unexplored. [12] It is a challenging work to obtain hybrids based on POMs and carboxylates. Obviously, also it is a challenging work to obtain hybrids constructed from POMs and TMMCs containing carboxylates.

We thus focused on the synthesis of type **3** compounds constructed from POMs and TMMCs of a N-containing ligand and a pyridinecarboxylate, which should be the breakthrough point for the synthesis of type **2** and type **3** compounds. The reason is that each pyridinecarboxylate not only is a N-containing ligand but also contains a carboxylate group; it will adopt both the coordination fashions of N-containing ligands and carboxylates. To synthesize this kind of compounds, we need to select a suitable N-containing ligand and a suitable pyridinecarboxylate. After searching the pyridinecarboxylates, we select nicotinic acid and its isomers as the candidates.

Fortunately, we successfully prepared five new complexes: $[Cu_3(2,2'\text{-bpy})_3(inic)(\mu_2\text{-}OH)(H_2O)][SiW_{12}O_{40}].2H_2O$ (**1**), $[Cu_6(phen)_6(\mu_3\text{-}Cl)_2(\mu_2\text{-}Cl)_2Cl_2(inic)_2][SiW_{12}O_{40}].6H_2O$ (**2**), $[Cu_2(hnic)(2,2'\text{-bpy})_2Cl]_2[H_2SiW_{12}O_{40}]$ (**3**), $[Cu_2(nic)(phen)_2Cl_2]_2[SiW_{12}O_{40}]$ (**4**) and $[Cu_2(pic)(2,2'\text{-bpy})_2Cl]_2[SiW_{12}O_{40}]$ (**5**). Single crystal X-ray analysis reveals that all the five compounds are based on the identical Keggin POM $[SiW_{12}O_{40}]^{4-}$ and different TMMCs. Compound **1** exhibits a 2-D double layer framework structure constructed from $[SiW_{12}O_{40}]^{4-}$ and copper-aqua-2,2'-bipy-hydroxyl-isonicotinate complexes. Compound **2** is a 0-D structure formed by $[SiW_{12}O_{40}]^{4-}$ and copper-chloro-isonicotinate-phenanthroline complexes. Compound **3** shows a 1-D chain structure based on $[SiW_{12}O_{40}]^{4-}$ linked by copper-2,2-bpy-chloro-2-hydroxy-nicotinate complexes. Compounds **4** and **5** show similar structures, which are a POM supported copper-chloro-nicotinate-phenanthroline complex in **4** and a POM supported copper-2,2-bpy-chloro-nicotinate complex in **5**. It should be noted that the nicotinic, isonicotinic and picolinic acid in compounds **1**, **2**, **4** and **5** are structural isomers and the 2-hydroxy-nicotinic acid in compound **3** is a hydroxylated product of the nicotinic acid.

Experimental

Materials and measurements

All the chemicals used were of reagent grade without further purification. Infrared spectra were recorded as KBr pellets on a Perkin-Elmer SPECTRUM ONE FTIR spectrophotometer. Reflection intensity data were collected on a Bruker Apex II diffractometer equipped with graphite monochromated Mo Kα (0.71073) radiation at room temperature, respectively. All the structures were solved by direct methods and refined using full-matrix least-squares on F^2 using the SHELXTL-97 crystallographic software package. XPS measurements were performed on single crystals with an ESCALAB MARK II apparatus, using the Mg Ka (1253.6 eV) achromatic X-ray radiation source. UV-vis spectra were recorded on a Shimadzu UV3100 spectrophotometer. Powder XRD patterns were obtained with a Scintag X1 powder diffractometer system using Cu Kα radiation with a variable divergent slit and a solid-state detector. The electrochemical measurements were carried out on a CHI 660B electrochemical workstation. The working electrode was a glassy carbon, while the surface of the glassy carbon working electrode was polished with 1μm alumina and washed with distilled water before each experiment. The counter electrode was a Pt wire and an Ag/AgCl was served as reference electrode. The measurements were made at room temperature of 25ºC.

Syntheses of compounds 1-5

Synthesis of $[Cu_3(2,2'\text{-bpy})_3(inic)(\mu_2\text{-}OH)(H_2O)][SiW_{12}O_{40}]\cdot 2H_2O$ (1) A mixture of $Na_2SiO_3\cdot 9H_2O$ (0.300g, 1.056mmol), $Na_2WO_4\cdot 2H_2O$ (0.669g, 2.028mmol),

Table 1. crystal data and structural refinements for compounds **1** - **5**.

Empirical formula	$C_{36}H_{35}Cu_3N_7O_{46}SiW_{12}$	$C_{84}H_{68}Cl_6Cu_6N_{14}O_{50}SiW_{12}$	$C_{52}H_{40}Cl_2Cu_4N_{10}O_{46}SiW_{12}$	$C_{60}H_{40}Cl_4Cu_4N_{10}O_{44}SiW_{12}$	$C_{52}H_{40}Cl_2Cu_4N_{10}O_{44}SiW_{12}$
Formula weight	3726.53	4901.69	4100.29	4235.19	4068.29
Crystal system	monoclinc	triclinic	monoclinc	triclinic	monoclinc
space group	P2(1)/c	P-1	P2(1)/n	P-1	P2(1)/c
a (Å)	23.4183(7)	11.702(2)	15.070(4)	12.186(2)	14.797(3)
b (Å)	12.9661(3)	14.419(3)	13.496(3)	12.977(3)	13.334(3)
c (Å)	22.7238(7)	18.071(4)	18.814(5)	14.887(3)	23.821(7)
α (˚)	90	71.19(3)	90	102.93(3)	90
β (˚)	109.508(2)	88.84(3)	90.953(4)	91.43(3)	126.20(2)
γ (˚)	90	80.19(3)	90	102.46(3)	90
Volume ($Å^3$)	6503.9(3)	2842(1)	3826(2)	2233.8(8)	3792.7(16)
Z	4	1	2	1	2
D_C ($Mg\cdot m^{-3}$)	3.806	2.864	3.559	3.148	3.562
μ (mm^{-1})	22.209	13.425	19.232	16.531	19.397
F(000)	6625	2247	3684	1907	3652
θ for data collection	0.92 to 28.35	3.02 to 27.49	1.86 to 25.84	1.65 to 25.94	2.99 to 27.48
Reflections collected	47065	27840	15229	16247	34560
Reflections unique	16161	12791	7252	8463	8628
R(int)	0.0988	0.0370	0.0397	0.0303	0.0590
Completeness to θ	99.5	98.2	98.1	97.2	99.3
parameters	946	799	593	629	584
GOF on F^2	1.009	1.007	1.054	1.007	1.063
R^a [I>2σ(I)]	$R_1 = 0.0447$	$R_1 = 0.0558$	$R_1 = 0.1076$	$R_1 = 0.1001$	$R_1 = 0.0894$
R^b (all data)	$\omega R_2 = 0.1164$	$\omega R_2 = 0.1295$	$\omega R_2 = 0.2304$	$\omega R_2 = 0.2181$	$\omega R_2 = 0.2051$

[a] $R_1 = \sum||F_o|-|F_c||/\sum|F_o|$. [b] $\omega R_2 = \{\sum[w(F_o^2-F_c^2)^2]/\sum[w(F_o^2)^2]\}^{1/2}$.

2,2'-bipy (0.079g, 0.506mmol), isonicotinic acid (0.063g, 0.512mmol),$CuSO_4 \cdot 5H_2O$ (0.499g, 2.000mmol) and H_2O (25ml) was stirred for 2 hours, adjust the starting pH value to 2 by the addition of 37% HCl solution, then adjust the pH value to 3 by the addition of $NH_3 \cdot H_2O$ solution, finally the suspension was transferred to a 50mL Teflon-lined reactor under autogenous pressure at 160ºC for 3 days. The autoclave was then cooled to room temperature. Blue block crystals were obtained, washed with distilled water and air-dried. Yield: 35% (based on W). Anal. calcd for $SiW_{12}O_{46}Cu_3C_{36}N_7H_{35}$: Si 0.75, W 59.20, Cu 5.12, C 11.60, N 2.63, H 0.95%; Found: Si 0.61, W 58.96, Cu 5.27, C 11.79, N 2.60, H 0.65%. IR (cm^{-1}): 3573, 3389, 3110, 2922, 2853, 1968, 1603, 1584, 1544, 1496, 1472, 1448, 1416, 1396, 1321, 1283, 1249, 1230, 1214, 1174, 1162, 1108, 1061, 1033, 1016, 981, 963, 922, 886, 795, 767, 535, 480, 418, 384, 336.

Synthesis of $[Cu_6(phen)_6(\mu_3\text{-}Cl)_2(\mu_2\text{-}Cl)_2Cl_2(inic)_2][SiW_{12}O_{40}]\cdot 6H_2O$ (2) Compound **2** was synthesized by using a similar experimental procedure as that of **1** except that Phen·H_2O (0.099g, 0.500mmol) and H_2O(15ml) were used instead of 2,2'-bipy and H_2O(25ml). Blue block crystals were obtained, washed with distilled water and air-dried. Yield: 22% (based on W). Anal. calcd for $SiW_{12}O_{50}Cu_6C_{84}N_{14}H_{68}C_{l6}$: Si 0.58, W 45.01, Cu 7.78, C 20.58, N 4.00, H 1.40; Found: Si 0.44, W 45.31, Cu 7.90, C 20.79, N 4.34, H 1.15%. IR (cm^{-1}): 3790, 3411, 3062, 2921, 1959, 1601, 1554, 1520, 1427, 1400, 1342, 1312, 1224, 1149, 1109, 1060, 1013, 974, 920, 884, 848, 791, 720, 530, 433, 386, 337.

Synthesis of $[Cu_2(hnic)(2,2'\text{-}bpy)_2Cl]_2[H_2SiW_{12}O_{40}]$ (3) Compound **3** was synthesized by using a similar experimental procedure as that of **1** except that nicotinic acid (0.062g, 0.509mmol) and H_2O(15ml) were used instead of isonicotinic acid (0.063g, 0.512mmol) and H_2O (25ml). Blue block crystals were obtained, washed with distilled water and air-dried. Yield: 27% (based on W). Anal. calcd for $C_{52}H_{40}Cl_2Cu_4N_{10}O_{46}SiW_{12}$: Si 0.68, W 53.81, Cu 6.20, C 15.23, N 3.42, H 0.98%; Found: Si 0.55, W 53.42, Cu 6.11, C 15.40, N 3.55, H 0.72%. IR (cm^{-1}): 3419, 3266, 3095, 3052, 2859, 1984, 1652, 1605, 1568, 1496, 1471, 1445, 1394, 1318, 1253, 1216, 1154, 1104, 1062, 1032, 1009, 960, 918, 878, 798, 727, 588, 535, 420, 385, 335.

Synthesis of $[Cu_2(nic)(phen)_2Cl_2]_2[SiW_{12}O_{40}]$ (4) Compound **4** was synthesized hydrothermally by reacting $Na_2SiO_3 \cdot 9H_2O$ (0.302g, 1.063mmol), $Na_2WO_4 \cdot 2H_2O$ (0.662g, 2.006mmol), nicotinic acid (0.062g, 0.509mmol), Phen (0.099g, 0.500mmol), $CuCl_2 \cdot 2H_2O$ (O.342g, 2.006mmol) and H_2O (15ml). The pH was adjusted to **2** with 37% HCl solution, and then adjusted to 4 by the addition of $NH_3 \cdot H_2O$ solution. Finally the suspension was transferred to a 50mL Teflon-lined reactor under autogenous pressure at 160ºC for 3 days. The autoclave was then cooled to room temperature. Blue block crystals were obtained, washed with distilled water and air-dried. Yield: 31% (based on W). Anal. calcd for $C_{60}H_{40}Cl_4Cu_4N_{10}O_{44}SiW_{12}$: Si 0.66, W, 52.09, Cu, 6.00, C 17.02, N 3.31, H 0.95%; Found: Si 0.52, W 51.83, Cu 5.88, C 17.17, N 3.14, H 0.69%. IR (cm^{-1}): 3786, 3507, 3185, 3129, 3087, 2952, 2880, 1942, 1739, 1641, 1615, 1585, 1517, 1414, 1340, 1224, 1186, 1152, 1109, 1014, 973, 920, 885, 848, 795, 718, 534, 477, 431, 384, 337.

Synthesis of $[Cu_2(pic)(2,2'\text{-}bpy)_2Cl]_2[SiW_{12}O_{40}]$ (5) Compound **5** was synthesized by using a similar experimental procedure as that of **4** except that picolinic acid (0.123g, 1.002mmol) and 2,2'-bipy (0.078g, 0.499mmol) were used instead of nicotinic acid (0.062g, 0.509mmol) and Phen (0.099g, 0.500mmol). Blue block crystals were obtained, washed with distilled water and air-dried. Yield: 41% (based on W). Anal. calcd for $C_{52}H_{40}Cl_2Cu_4N_{10}O_{44}SiW_{12}$: Si 0.69, W 54.23, Cu 6.25, C 15.35, N 3.44, H 0.99%; Found: Si 0.56, W 53.11, Cu 6.00, C 15.03, N 3.06, H 0.57%. IR (cm^{-1}): 3425, 3114, 3062, 2922, 1979, 1639, 1603, 1568, 1472, 1445, 1414, 1321, 1249, 1154, 1104, 1009, 961, 918, 877, 798, 773, 758, 728, 539, 479, 421, 385, 336.

X-ray crystallography

The reflection intensity data for compound **1** were measured on a Bruker Apex II diffractometer with graphite monochromated Mo K_α (λ = 0.71073Å) radiation. The reflection intensity data for compounds **2** and **5** were measured on a Rigaku R-AXIS RAPID diffractometer with graphite monochromated Mo K_α (λ = 0.71073Å) radiation, and the reflection intensity data for compounds **3** and **4** were measured on an Agilent Technology SuperNova Eos Dual system with a Cu-Kα (λ = 1.54184Å) microfocus source and focusing multilayer mirror optics. None of the crystals showed evidence of crystal decay during data collections. The five structures were solved by direct methods and refined using the full-matrix least squares on F^2 with the SHELXTL-97 crystallographic software package. In the final refinements, all atoms were refined anisotropically in compounds **1**-**5**, while those of water molecules in compound **1** and **2** were not added. The maxima and minima residual electron density for compounds **3, 4** and **5** are 3.60, -2.69, 3.07, -4.93 and 3.79, 3.04e·Å^{-3}, respectively, the locations of the maximum and the minimum are about 1.80Å from O(12), 1.64Å from O(20) for compound **3,** 0.99Å from W(4), 0.89Å from C(18) for compound **4**, and 0.69Å from O(5), 1.59Å from N(4) for compound **5**, respectively. A summary of the crystallographic data and structure refinements for compounds **1**-**5** is given in Table **1**. Selected important bond distances were listed in Table s1. CCDC number: 967747 for **1,** 967748 for **2,** 967749 for **3,** 967750 for **4** and 967751 for **5**. These data can be obtained free of charge from The Cambridge Crystallographic Data Centre *via* www.ccdc.cam.ac.uk/data_request/cif.

Results and discussion

Synthesis

The five compounds are respectively synthesized by using a rigid N-heterocyclic ligand and a pyridinecarboxylate. Compounds **1**-**3** were synthesized under very similar conditions: identical pH values, identical temperatures, identical reaction times, identical starting materials, identical molar ratios, except for N-heterocyclic ligands and pyridinecarboxylates, as shown in Scheme 1. However, the structures of the three compounds are thoroughly different. The final structures were not only affected by different N-heterocyclic ligands and pyridinecarboxylates, but also affected by chloride ions added for the adjustments of pH values. It is clear that chloride ions in compounds **2** and **3** come from the 37% HCl solution.

We speculate that chloride ions perhaps will play an important role in the formations of such compounds. Therefore, we used $CuCl_2$ replacing $CuSO_4$. And then, we got compounds **4** and **5**, it is noted that the two compounds are similar, both of which exhibit a POM supported transition metal complex structure. The two supported transition metal complexes in compounds **4** and **5** are different, which comes from the different coordination fashions of the nicotinate and picolinate ligands.

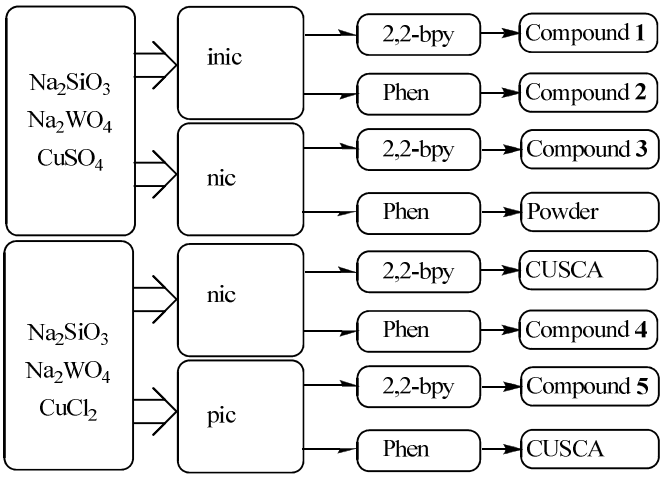

Scheme 1. Summary of the reactions of compounds **1-5**. CUSCA means crystals unsuitable for single crystal analysis.

As shown in Scheme 1, attempts to synthesize a new compound using the identical procedure to that of compound **3** except for replacing 2,2-bpy by Phen have already been tried. However, we only got some unidentified powders. In addition, attempts to synthesize new compounds using identical procedures to those of compounds **4** and **5** except for replacing Phen by 2,2-bpy and replacing 2,2-bpy by Phen have already been respectively tried too. However, these attempts only give rise to some poor-quality crystals which are unsuitable for single crystal analysis.

To the best of our knowledge, coordination modes of inic ligands can be grouped into five different types,[13] as shown in scheme 2 (1a to 1e), the most common types are 1a and 1c. The coordination mode of inic in both compounds **1** and **2** is 1d. Therefore, the different final structures of compounds **1** and **2** perhaps come from the different steric hindrance of the two different chelating ligands. In addition, the coordination complexes based on copper and inic (compounds **1** and **2**) adopting such a coordination mode are observed for the first time.

In addition, one interesting feature of compound **3** is that nic acids transform to hnic acids via *in situ* hydroxylation. A variety of novel hybrid complexes involving *in situ* synthesized ligands were documented. To date, more than 10 types of ligand *in situ* formation reactions have been reported, including carbon-carbon bond formation, hydroxylation, ether bond formation, decarboxylation, tetrazole and triazole formation, alkylation, hydrolysis, transformation between inorganic sulfur and organic sulfur, acylation and isomerization. [14] The starting material is nic acids. However, the organic component in the resulting hybrid becomes a hnic group. Hydroxylation of nic acids leading to hnic groups in compound **3**, which was not documented previously, is the result of nucleophilic attack of hydroxide ions.

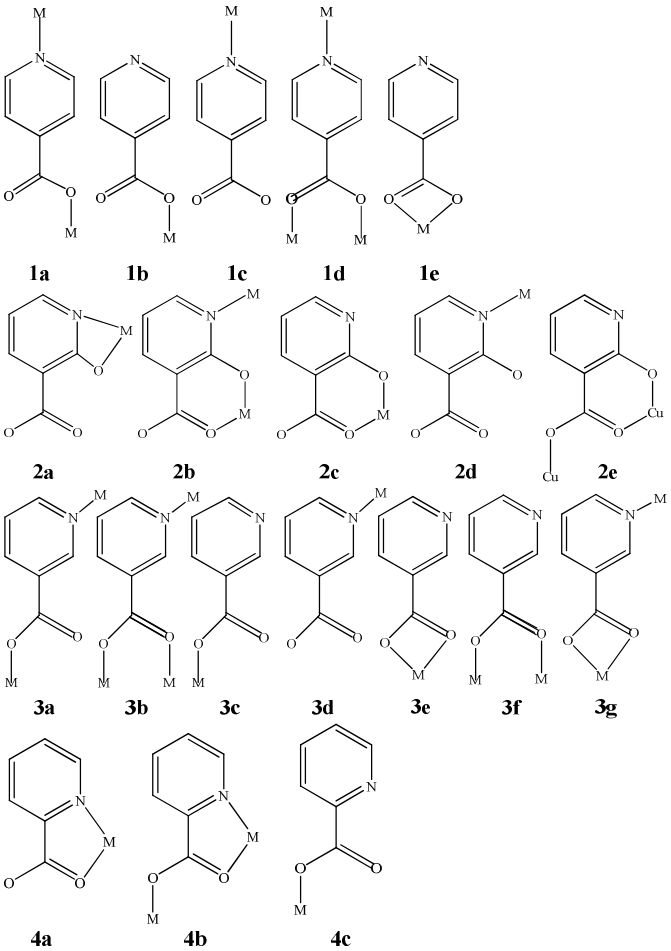

Scheme 2. (1a-1e) Five coordination modes of inic ligands; (2a-2d) four coordination modes of hnic ligands; (3a-3g) seven coordination modes of nic ligands; (4a-4c) three coordination modes of pic ligands; and coordination modes of organic ligands in compounds **1-5.**

Coordination fashions of hnic ligands can be classified into four types, [15] as shown in scheme 2 (2a to 2d). The hnic ligand in compound **3** adopts an unprecedented type of coordination mode to bind two copper ions (scheme 2 (2e)): one carboxylate oxygen and the hydroxyl oxygen of each hnic ligand in compound **3** form a most stable six-membered chelate ring with a copper ion, whereas the other carboxylate oxygen coordinates to another copper ion. The reason that the nitrogen atom of the hnic ligand did not coordinate to any cooper ions perhaps originates from the steric hindrance in compound **3**.

The coordination modes of nic ligand is more diverse (scheme 2 (3a to 3g)). [16] The nic ligand in compound **4** adopts the sixth coordination mode with its two carboxylate oxygens coordinating to two coppers respectively (scheme 2 (3f)).

Pic ligands exhibits three coordination modes (scheme 2 (4a to 4c)). [17] The pic ligand in compound **5** adopts the second one (scheme 2 (4b)). The coordination mode of the pic ligand in compound **5** is similar to that of hnic in compound **3**, though the two ligands are different. One carboxylate oxygen and the nitrogen of the pic ligand in compound **5** form a stable five-membered chelate ring with a copper ion, whereas the other carboxylate oxygen coordinates to another copper ion, as shown in Scheme 2 (4b).

Description of the crystal structures

Crystal structure of 1 The five compounds were investigated by single crystal X-ray analysis, which reveals that all the POMs of the five compounds are the Keggin polyoxoanion $[SiW_{12}O_{40}]^{4-}$. The POM in compound **1** was detailedly described below as an example. The structure of the Keggin core in compound **1** is unexceptional, including a central $\{SiO_4\}$ tetrahedron surrounded by twelve $\{WO_6\}$ octahedra arranged in four groups of three edge-sharing octahedra units $\{W_3O_{13}\}$. According to different coordination fashions, W-O bonds can be classified into three sets: W-O_t (terminal oxygens) with distances of 1.67(1)-1.72(1)Å, W-O_b (bridging oxygens) with distances of 1.87(1)-1.97(1)Å and W-O_c (central oxygens) with distances of 2.335(8)-2.369(8)Å. Oxidation states for the W atoms in compound **1** were calculated using the parameters given by Brown.[18] Results indicate that all the tungsten atoms are in the +6 oxidation state.

X-ray analysis of a single crystal of compound **1** shows that its asymmetric unit is composed of a polyoxoanion $[SiW_{12}O_{40}]^{4-}$, a copper-aqua-2,2'-bipy-hydroxyl-isonicotinate complex $[Cu_3(2,2'\text{-bipy})_3(inic)(H_2O)(OH^-)]^{4+}$ and two water molecules. The complex $[Cu_3(2,2'\text{-bipy})_3(IN)(H_2O)(OH^-)]^{4+}$ in compound **1** consists of three crystallographically independent Cu^{2+} centers, three 2,2'-bipy, an inic ion, a water molecule and a hydroxyl ion. N(1), N(3) and N(5) 2,2'-bipy ligands form three stable chelates with Cu(1), Cu(2) and Cu(3) with Cu-N distances of 1.97(1)-2.01(1)Å. The two carboxylate oxygens (O(42) and O(43)) of the inic ligand respectively coordinate to Cu(1) and Cu(2) with Cu-O distances of 1.955(9)-1.97(1)Å, indicating that the inic ligand joins the two copper ions. The distance of Cu(1) and Cu(2) is 3.289(2)Å, indicating little, if any, direct metal-metal interaction between the two copper ions. N(7) of the inic ligand coordinates to Cu(3) with a Cu-N distance of 2.03(1)Å. Thus, the inic ligand acting as a μ_3-bridge links the three crystallographically independent Cu^{2+} centers of $[Cu_3(2,2'\text{-bipy})_3(inic)(H_2O)(OH^-)]^{4+}$. O(41) of the hydroxyl group coordinates to Cu(1) and Cu(2) with Cu-O distances of 1.88(1)-1.91(1)Å. It should be noted that the Cu-O distances are shorter, confirming that O(41) is a hydroxyl oxygen. The role of Ow(1) in $[Cu_3(2,2'\text{-bipy})_3(inic)(H_2O)(OH^-)]^{4+}$ is a terminal ligand coordinating to Cu(3) with a Cu-O distance of 1.97(1)Å. In one word, the inic ligand plays the most important role for the formation of $[Cu_3(2,2'\text{-bipy})_3(inic)(H_2O)(OH^-)]^{4+}$, which links three $[Cu(2,2'\text{-bipy})]^{2+}$ chelates into a TMMC.

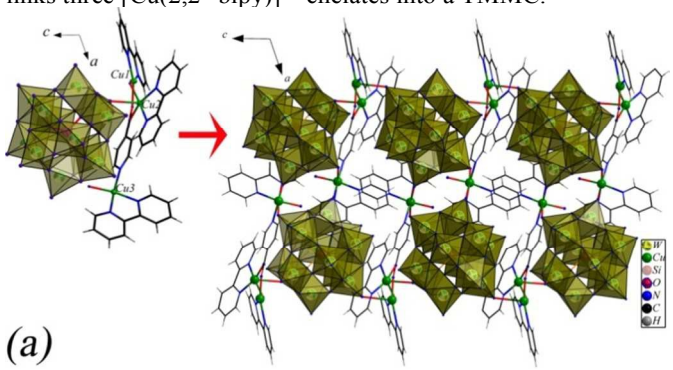

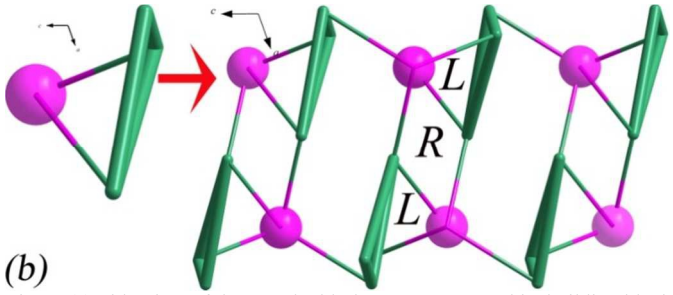

Fig. 1. (a) Side-view of the 2-D double-layer structure and its building block in compound **1**; (b) topological representation of the 2-D double-layer structure and its building block in compound **1**.

Each $[Cu_3(2,2'\text{-bipy})_3(inic)(H_2O)(OH^-)]^{4+}$ exhibits covalent interactions with surrounding POMs via contacts between its coppers and POM oxygens. As shown in Fig. 1, Cu(1) and Cu(2) of $[Cu_3(2,2'\text{-bipy})_3(inic)(H_2O)(OH^-)]^{4+}$ each interact with one POM with Cu-O distances of 2.63(1) and 2.46(1)Å, whereas Cu(3) of $[Cu_3(2,2'\text{-bipy})_3(inic)(H_2O)(OH^-)]^{4+}$ interacts with another two POMs with Cu-O distances of 2.50(1)-2.54(1)Å. That is to say, Cu(3) acts as a μ_2-bridge linking two POMs, whereas Cu(1) and Cu(2) are each supported by one POM. Therefore, each TMMC acting as a μ_4-bridge connects four POMs. On the other hand, each POM in compound **1** serves as a multidentate ligand coordinating to one Cu(1), one Cu(2) and two Cu(3) from four TMMCs, indicating that each POM acting as a μ_4-bridge joins four TMMCs. Thus, through Cu-O contacts between POMs and TMMCs, a 2-D double-layer structure has been formed as shown in Fig. 1.

To get a better insight into the present 2-D framework structure, a topological analysis was carried out for compound **1**. Each $[Cu_3(2,2'\text{-bipy})_3(inic)(H_2O)(OH^-)]^{4+}$ can be represented by a triangle, which connects four POMs, and can be regarded as a 4-connected triangle. Each POM connects four $[Cu_3(2,2'\text{-bipy})_3(inic)(H_2O)(OH^-)]^{4+}$, and can be treated as a 4-connected node. Such connectivity repeats infinitely to give the 2-D framework as shown in Fig. 1. It should be noted that there exist two trigonal L-helical tubes and a rhombic R-helical tube in the 2-D framework. As shown in Fig. 1(b), the two trigonal L-helical tubes are linked to the rhombic R-helical tube by sharing edges. Except for the three helical tubes in the 2-D framework, there exist a 1-D tube which is formed by two POMs and two $[Cu_3(2,2'\text{-bipy})_3(inic)(H_2O)(OH^-)]^{4+}$, however, the detailed analysis reveals that this tube is not a helical one. Thus, a 2-D framework structure linked by helical tubes and unhelical tubes alternately was formed (Fig. 1).

The crystal analysis strongly suggests the existence of C-H···O interactions between carbon atoms of copper-aqua-2,2'-bipy-hydroxyl-isonicotinate complexes and oxygen atoms of POMs. C···O Distances of C-H···O interactions are listed in table s2. The 2-D double layers were linked by these C-H···O interactions into a 3-D supramolecular structure.

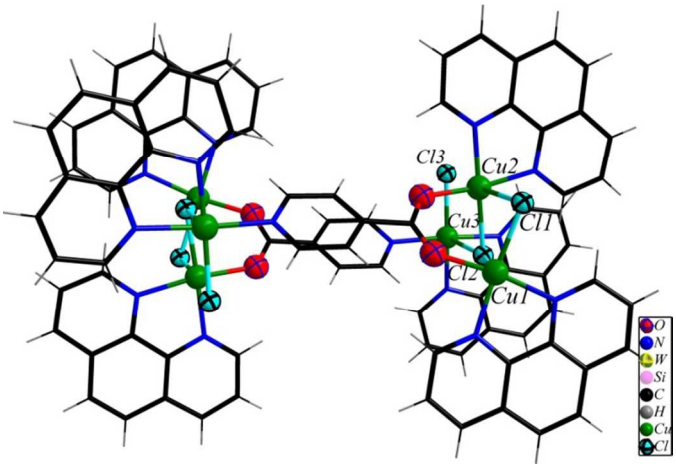

Fig. 2. Ball-and-stick and wire representation of the copper-chloro-isonicotinate-phenanthroline complex in compound **2**.

Crystal structure of 2 The asymmetric unit of compound **2** consists of half a $[SiW_{12}O_{40}]^{4-}$ polyoxoanion, half a copper-chloro-isonicotinate-phenanthroline complex $[Cu_6(Phen)_6(\mu_3\text{-}Cl)_2(\mu_2\text{-}Cl)_2Cl_2(inic)_2]^{4+}$ and three water molecules. $[Cu_6(Phen)_6(\mu_3\text{-}Cl)_2(\mu_2\text{-}Cl)_2Cl_2(inic)_2]^{4+}$ with an inversion center, is comprised of two Cu(1), two Cu(2), two Cu(3), two N(1), two N(3) and two N(5) Phen ligands, two Cl(1), two Cl(2) and two Cl(3) and two inic ions. The copper-chloro-isonicotinate-phenanthroline complex presents a discrete coordination structure.

Both crystallographically independent Cu(1) and Cu(2) in $[Cu_6(Phen)_6(\mu_3\text{-}Cl)_2(\mu_2\text{-}Cl)_2Cl_2(inic)_2]^{4+}$ adopt a distorted square pyramidal geometry with two Phen nitrogens, one chloride ion and one carboxylate oxygen from an inic ligand forming the basal plane, and with another chloride ion at the vertex. Cu-N distances of the two copper complexes are in the range of 2.00(1)-2.03(1)Å, Cu-O distances range from 1.944(9) to 1.979(9)Å, and Cu-Cl distances are 2.258(4)-2.757(4)Å. It should be noted that Cu(1) and Cu(2) are not only linked by two chloride ions but also linked by an inic ligand into a dimer, as shown in Fig. 2. The geometry around Cu(3) is slightly different from those around Cu(1) and Cu(2), the coordination sites in the basal plane of Cu(3) pyramid are occupied by two Phen nitrogens, one nitrogen from an inic ligand and one chloride ion, the vertex of the square pyramid is occupied by another chloride ion. Cu-N, Cu-O and Cu-Cl distances of Cu(3) complex are all comparable to those of Cu(1) and Cu(2) complexes. It is clear that the main difference of Cu(3) and Cu(1) (or Cu(2)) pyramids is that one inic nitrogen atom takes the place of one inic carboxylate oxygen atom in the basal plane. Cu(2) and Cu(3) square pyramids are joined by sharing-vertex, and Cu(1) and Cu(2) square pyramids are joined by sharing-edge. On the other hand, Cl(1) acting as a μ_2-bridge coordinates to both Cu(1) and Cu(2), Cl(2) as a μ_3-bridge joins all the three crystallographically independent copper ions, while Cl(3) serving as a terminal ligand only coordinates to Cu(3). Therefore, Cl(2) plays the most important role in the formation of the copper-chloride cluster in $[Cu_6(Phen)_6(\mu_3\text{-}Cl)_2(\mu_2\text{-}Cl)_2Cl_2(inic)_2]^{4+}$.

There are two such copper-chloride clusters joined by two N(7) inic ligands into the discrete complex $[Cu_6(Phen)_6(\mu_3\text{-}Cl)_2(\mu_2\text{-}Cl)_2Cl_2(inic)_2]^{4+}$ in compound **2**. Each inic ligand adopting the end-to-end coordination mode is μ-bonded to three Cu^{2+} with the longest Cu···Cu separation of 5.389(1)Å.

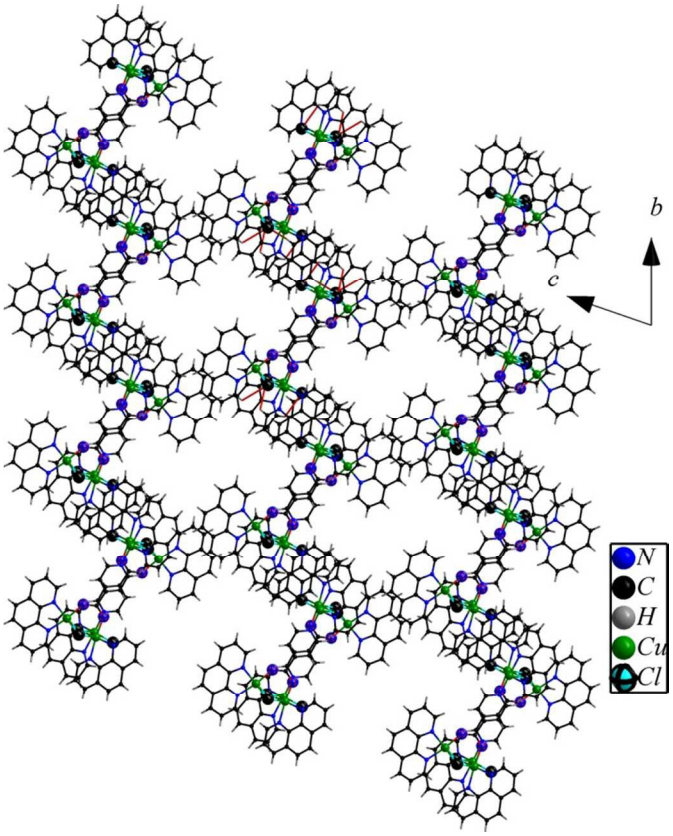

Fig. 3. The 3-D supramolecular packing structure of compound **2** viewed along the a axis.

Compound **2** contains C-H···Cl interactions which play an important role in the formation of the supramolecular structure of compound **2**. As shown in Fig. 3, C-H···Cl interactions in compound **2** can be classified into two types, the first type can be described as intramolecular C-H···Cl interactions, which includes C(10)-H(10)···Cl(1), C(13)-H(13)···Cl(2), C(25)-H(25)···Cl(3) and their symmetry equivalents. C-Cl distances are 3.261(1)-3.329(1)Å, H-Cl distances are 2.6939(9)-2.794(1)Å and C-H···Cl angles are 117.63(3)-120.13(3)º. The second type can be described as intermolecular C-H···Cl interactions, which includes C(18)-H(18)···Cl(1) and its symmetry equivalents with a C-Cl distance of 3.726(1)Å, H-Cl distance of 2.8317(8)Å and C-H···Cl angle of 161.74(4)º. Through intermolecular C-H···Cl interactions, copper-chloro-isonicotinate-phenanthroline complexes are linked into a 1-D supramolecular chain structure propagating along the (1,-1, 0) direction (Fig. s2). 1-D supramolecular chains are arranged into a 3-D supramolecular structure with large oval channels of approximately 19.029(6)×10.172(3)Å viewed along the *a* axis, as shown in Fig. 3. It should be noted that the channels are supported by POMs via C-H···O interactions, which are listed in table s2.

Crystal structure of 3. The asymmetric unit of compound **3** comprises half a $[SiW_{12}O_{40}]^{4-}$ polyoxoanion and a copper-2,2-bpy-chloro-2-hydroxy-nicotinate complex $[Cu_2(hnic)(2,2'\text{-}bipy)_2Cl]^{+}$. It should be noted that two hydrogen atoms should be added to the POM anion to balance the charge of the anion. The complex $[Cu_2(hnic)(2,2'\text{-}bipy)_2Cl]^{+}$ in compound **3** is composed of two crystallographically independent copper ions, two 2,2-bpy, a chloride ion and a hnic ligand. N(1) and N(3) 2, 2-bpy adopting the N, N-chelating mode respectively coordinate to Cu(1) and Cu(2) with Cu-N distances of 1.98(3)-2.00(3)Å. Cl(1) coordinates to Cu(2) with a Cu-Cl distance of

2.24(1)Å. Both the hydroxyl oxygen and one carboxylate oxygen of hnic are simultaneously bound to Cu(1) with Cu-O distances of 1.90(2)-1.94(2)Å, while the other carboxylate oxygen of hnic is bonded to Cu(2) with a Cu-O distance of 1.94(2)Å. The hnic ligand adopting the end-to-end coordination mode joins the two crystallographically independent Cu^{2+} ions into a TMMC with a Cu···Cu separation of 5.2141(9)Å. It should be noted that the hnic ligand contains a nitrogen atom which did not coordinate to any copper ions. We speculate that the reason should be due to the steric hindrance.

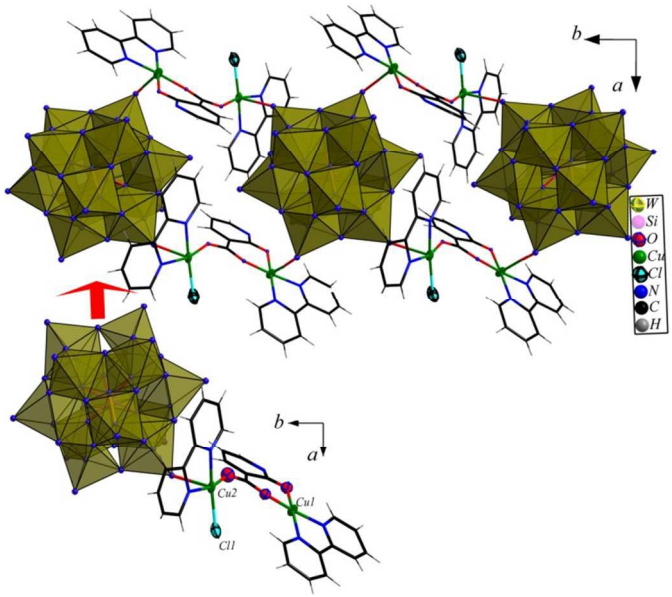

Fig. 4. Polyhedral and wire representation of the 1-D chain structure in compound **3**.

Cu(2) of $[Cu_2(hnic)(2,2'\text{-bipy})_2Cl]^+$ exhibits a covalent interaction with a POM with a Cu-O distance of 2.5549(4)Å, whereas Cu(1) of $[Cu_2(hnic)(2,2'\text{-bipy})_2Cl]^+$ interacts with another POM via a weak Cu-O interaction with a Cu-O distance of 2.8318(4)Å. Through contacts between Cu(1) and Cu(2) of $[Cu_2(hnic)(2,2'\text{-bipy})_2Cl]^+$ and oxygens from POMs, each $[Cu_2(hnic)(2,2'\text{-bipy})_2Cl]^+$ acting as a μ_2-bridge links POMs into a 1-D chain structure propagating along the *b* axis. Alternatively, each POM acts as a μ_4-bridge interacting with two Cu(1) and two Cu(2) from two $[Cu_2(hnic)(2,2'\text{-bipy})_2Cl]^+$ to form a 1-D chain as shown in Fig. 4. Further investigation of the structure shows that there exist C-H···O interactions which link the 1-D chains into a 3-D supramolecular structure, the C-H···O interactions are listed in table s2.

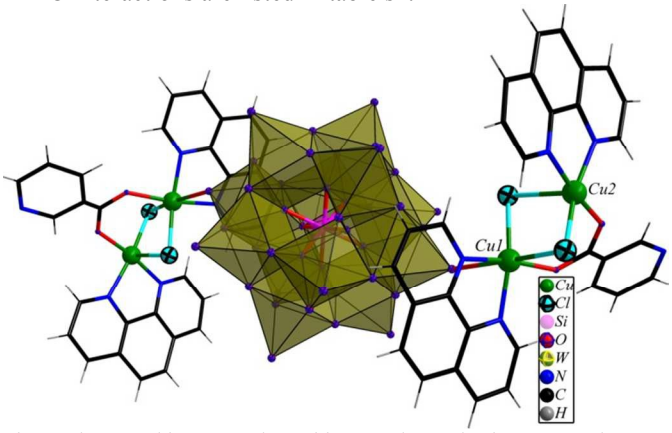

Fig. 5. The POM bi-supported transition metal complex in compound **4**.

Crystal structure of 4. The asymmetric unit of **4** is comprised of half a $[SiW_{12}O_{40}]^{4-}$ polyoxoanion and a copper-chloro-nicotinate-phenanthroline complex $[Cu_2(nic)(Phen)_2(Cl)_2]^+$. The complex $[Cu_2(nic)(Phen)_2(Cl)_2]^+$ consists of two crystallographically independent copper ions, two chloride ions and a nic ligand. As shown in Fig. 5, the two Phen respectively coordinate to Cu(1) and Cu(2) in a N, N-chelating mode with Cu-N distances of 1.99(2)-2.03(2)Å. The two chloride ions each connect Cu(1) and Cu(2) with Cu-Cl distances of 2.250(8)-2.812(9)Å acting as two μ_2-bridges. The nic ligand links the two copper ions via its two carboxylate oxygens with Cu-O distances of 1.95(2)-1.96(2)Å. Therefore, both the chloride ions and nic ligand play the fatal role for the formation of the TMMC in compound **4**.

Different from the coppers of TMMCs in compounds **1** and **3**, there is only one copper ion Cu(1) of the TMMC in compound **4** interacting with a POM with a Cu-O distance of 2.59(2)Å, Cu(2) exhibits no interactions with any POMs. That is to say, the complex $[Cu_2(nic)(Phen)_2(Cl)_2]^+$ is supported by a POM via the Cu-O contact to form a POM supported TMMC.

It should be noted that each two such TMMCs is disposed at the two opposite sides of a POM, which means that the POM act as a bidentate ligand coordinating to two Cu(1) from two $[Cu_2(nic)(Phen)_2(Cl)_2]^+$ to form a POM bi-supported TMMC, as shown in Fig. 5. There exist intramolecular C-H···Cl hydrogen bonding interactions in POM bi-supported TMMCs, which are C(13)-H(13)···Cl(2), C(1)-H(1)···Cl(1) and their symmetry equivalents with C-Cl distances of 3.303(2)-3.3118(8)Å, H-Cl distances of 2.761(1)-2.7552(7)Å and C-H-Cl angles of 118.14(5)-119.36(4)º.

Detailed analysis reveals that there also exist intermolecular C-H···Cl hydrogen bonding interactions. As shown in Fig. s3, Cl(1) is hydrogen-bonded to C(20) (3-x, 1-y, 1-z) with a C-Cl distance of 3.557(1)Å, H-Cl distance of 2.6593(9)Å and C-H-Cl angle of 162.47(7)º, indicating a strong C-H···Cl hydrogen bonding interaction. Through these C-H···Cl interactions, POM bi-supported TMMCs were linked into a 1-D chain structure running along the (1, 0, -1) direction.

Except for C-H···Cl hydrogen bonding interactions, the structure of compound **4** also contains complex C-H···O hydrogen bonding interactions, which are listed in table s2. Via the C-H···O interactions, the 1-D chains were linked into a 3-D supramolecular structure.

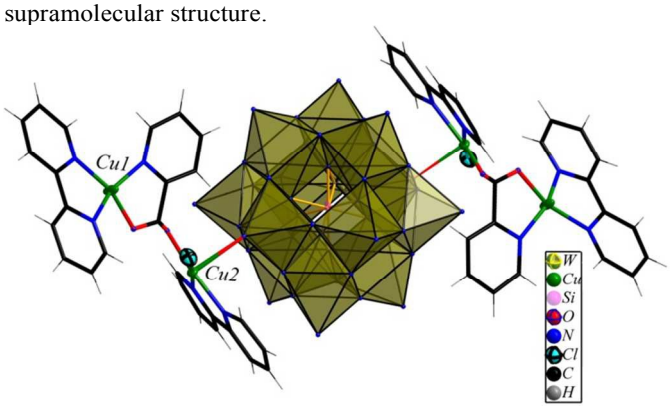

Fig. 6. The POM bi-supported transition metal complex in compound **5**.

Crystal structure of 5. The asymmetric unit of **5** consists of half a $[SiW_{12}O_{40}]^{4-}$ polyoxoanion and a copper-2,2-bpy-chloro-picolinate complex $[Cu_2(pic)(2,2\text{-bpy})_2Cl]^{2+}$. Compared with compound **4**, it is very clear that the composition and structure of compound **5** are very similar to those of compound **4** except that 2, 2-bpy and pic replace Phen and nic. The $[Cu_2(pic)(2,2\text{-bpy})_2Cl]^{2+}$ in compound **5** comprises two crystallographically

independent copper ions, two 2,2-bpy ligands, a chloride ion and a pic group. Like the roles of Phen in compound **4**, 2, 2'-bpy ligands in $[Cu_2(pic)(2,2\text{-}bpy)_2Cl]^{2+}$ serve as terminal ligands coordinating to the two crystallographically independent copper ions in a N, N-chelating mode. Different from the chloride ions in compound **4**, the chloride ion of $[Cu_2(pic)(2,2\text{-}bpy)_2Cl]^{2+}$ in compound **5** only serves as a terminal ligand coordinating to a copper ion. The coordination mode of pic in $[Cu_2(pic)(2,2\text{-}bpy)_2Cl]^{2+}$ is also different from that of nic in compound **4**, it not only coordinates to Cu(1) in a N, O-chelating fashion but also coordinates to Cu(2) in a monodentate fashion. That is to say, only pic ligand plays the most important role in the formation of the TMMC in compound **5**.

There is also only one copper ion of $[Cu_2(pic)(2,2\text{-}bpy)_2Cl]^{2+}$ exhibiting a covalent interaction with its neighboring POM just like the copper ion of the TMMC in compound **4**: Cu(2) of $[Cu_2(pic)(2,2\text{-}bpy)_2Cl]^{2+}$ interacts with a POM with a Cu-O distance of 2.42(2)Å. Through the contact between the copper ion and the POM oxygen, $[Cu_2(pic)(2,2\text{-}bpy)_2Cl]^{2+}$ is supported by a POM into a POM supported metal complex (Fig. 6).

Each two $[Cu_2(pic)(2,2\text{-}bpy)_2Cl]^{2+}$ is also disposed at the opposite sides of a POM to form a POM bi-supported metal complex. There also exist intramolecular C-H···Cl hydrogen bonding interactions in POM bi-supported complexes, which are C(20)-H(20)···Cl(1) and its symmetry equivalent with the C-Cl distance of 3.3301(8)Å, H-Cl distance of 2.7607(6)Å and C-H-Cl angle of 120.46(3)º.

Unfortunately, there do not exist intermolecular C-H···Cl hydrogen bonding interactions just like those in compound **5**. However, the detailed analysis reveals that compound **5** contains complex C-H···O hydrogen bonding interactions, which play a very important role in the formation of compound **5**. As shown in Fig. 7, C(4) and C(7) of the POM bi-supported complex are hydrogen-bonded to O(18a, a:2-x, -y, 1-z) and O(6a, a:2-x, -y, 1-z) from a neighboring POM bi-supported complex with C-O distances of 3.1271(6)-3.1802(7)Å and C-H-O angles of 107.83(3)-147.15(3)º, respectively. Therefore, via these C-H···O interactions, POM bi-supported complexes were linked into a 1-D supramolecular chain structure running along the (1, 1, 0) direction. The neighboring chains running along the (1, 1, 0) direction propagate along the *ab* plane into a 2-D supramolecular layer structure via a very weak Cu(1)-O(16a, a: x, 1+y, z) contact with a Cu-O distance of 3.0536(6)Å. Thus, a 2-D layer structure along the *ab* plane was formed by the 1-D chains stacked along the (1, -1, 0) direction.

The most unusual feature of compound **5** is that the two neighboring 2-D layers were formed by two identical chains with two different propagating directions: one is running along the (1, 1, 0) direction, while the other is running along the (1, -1, 0) direction. It should be noted that the two neighboring identical chains of the two layers with different propagating directions interact with each other via C(18)-H(18)···O(5a, a: 3-x, 0.5+y, 1.5-z) and C(19)-H(19)···O(23a, a: 3-x, 0.5+y, 1.5-z) hydrogen bonding interactions with C-O distances of 3.0197(9)-3.1057(8)Å and C-H-O angles of 93.93(3)-98.64(3)º. Thus, via the interweaving of the chains with different directions, a 3-D supramolecular structure was formed.

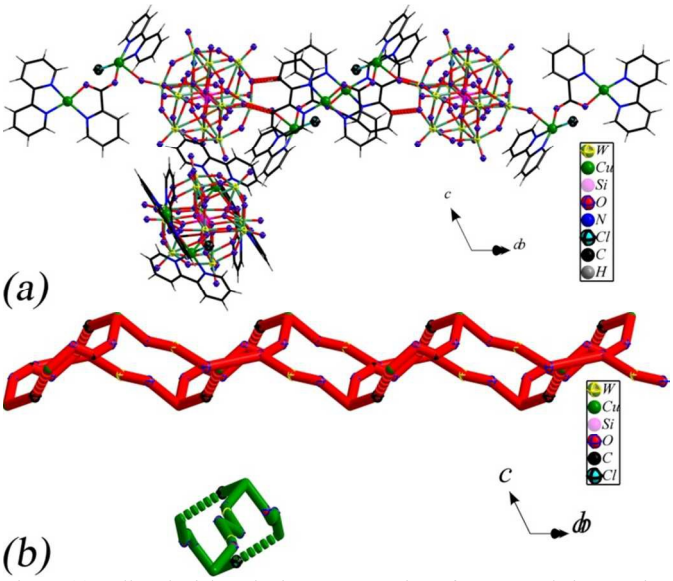

Fig. 7. (a) Ball-and-stick and wire representation of two 1-D chains running along the (1, 1, 0) and (1, -1, 0) directions. (b) Topological representation of the packing structure of compound **5**. The chain runs along the (1, 1, 0) direction is in red, and the chain runs along the (1, -1, 0) direction is in blue.

FT-IR spectra

Compounds **1-5** contain the identical Keggin POM $[SiW_{12}O_{40}]^{4-}$, therefore, the IR spectra of them are very similar. The IR spectrum of compound **1** was detailedly described below as an example. The IR spectrum of compound **1** is shown in Fig. s1, of which the characteristic band at 963cm^{-1} is attributed to $\upsilon(W\text{-}O_t)$, the band at 886 cm^{-1} is ascribed to $\upsilon(W\text{-}O_b\text{-}W)$, and the band at 795cm^{-1} is due to $\upsilon(W\text{-}O_c)$, respectively. The stretching of Si-O bonds is observed at the spectrum band of 922cm^{-1}.[19] The absorption bands at 1603-1108cm^{-1} are due to vibrations of bpy and isonicotinate ligands in compound **1**. The IR spectra of compounds **2-5** are similar to that of compound **1**. They exhibit characteristic bands at 974, 920, 884, 791cm^{-1} for **2**, 960, 918, 878, 798cm-1 for **3**, 973, 920, 885, 795cm^{-1} for **4** and 961, 918, 877, 798cm^{-1} for **5** ascribed to $\upsilon(W\text{-}O_t)$, $\upsilon(Si\text{-}O_c)$, $\upsilon(W\text{-}O_b\text{-}W)$ and $\upsilon(W\text{-}O_c)$, respectively,[19] while bands from 1601-1109cm^{-1}, 1652-1104cm^{-1}, 1641-1109cm^{-1} and 1639-1104cm^{-1} are assigned to Phen, isonicotinate in compound **2**, 2,2'-bipy, 2-hydroxy-nicotinate in compound **3**, Phen, nicotinate in compound **4** and 2,2'-bipy, picolinate in compound **5**, respectively.

XRD patterns

The X-ray powder diffraction patterns of compounds **1-5** are all in good agreement with the simulated XRD patterns, confirming the phase purity of all the five compounds (Fig. s2). The differences in reflection intensities are probably due to preferential orientations in the powder samples of compounds **1-5**.

XPS spectra

Fig. s3 shows the XPS spectrum of tungsten atoms in compound **1** with two peaks at 35.8eV and 37.8eV ascribed to W^{6+} 4f7/2 and W^{6+} 4f5/2. Compounds **1-5** contain the identical Keggin POM, therefore, the XPS spectra of tungsten atoms in compounds **2-5** are similar to those of compound **1**, which exhibit two peaks at 35.2eV, 37.4eV, 35.9eV, 38.1eV, 35.9eV,

38.1eV, and 35.8eV, 38.0eV, respectively, we assigned these to sites of W^{6+} in compounds **2-5**.

The Cu 2p3/2 peaks of compounds **1** are shown in Fig. s4, and exhibit the known characteristics of Cu^{2+}. The main peak of Cu^{2+} is relatively broad (about 3.4eV), has a binding energy of 935.1eV, and is accompanied by a satellite peak on the high-binding energy side at about 9eV.[20] Compounds **1-5** all contains Cu^{2+} cations, thus XPS spectra of compounds **2-5** are similar to that of compound **1**, which exhibit the characteristic peaks of Cu^{2+} cations at 934.3eV, 935.0eV, 934.8eV and 935.1eV in compounds **2-5**, and all of which are accompanied by satellite peaks on the high-binding energy side at about 9eV, respectively.

UV-Vis spectra

UV-Vis spectra of compounds **1-5**, in the range of 250-400 nm, are presented in Fig. s5. The UV-Vis spectrum of compound **1** displays an intense broad absorption peak centered about 260nm with two shoulder peaks at about 302 and 313nm assigned to O→W charge transfer and $n\rightarrow\pi^*$ transitions of 2, 2'-bpy and inic ligands in compound **1**. The UV-Vis spectra of compounds **4** and **5** exhibit very similar intense broad absorption peaks and shoulder peaks to compound **1** centered about 257, 303, 314 and 263, 302, 314nm, respectively, which should be ascribed to transfer bands of O→W and $n\rightarrow\pi^*$ transitions of organic ligands in compounds **4-5**. However, the UV-Vis spectra of compounds **2** and **3** show some difference from those of compounds **1**, **4** and **5** which exhibit peaks and shoulder peaks at 252, 274, 296 and 253, 272, 295nm, respectively, which should also be due to the transfer bands of O→W and $n\rightarrow\pi^*$ transitions of organic ligands.

Cyclic voltammograms

Fig. s6 shows cyclic voltammogram of the DMSO solution of compound **1** in the mixture of 0.5mol/L H_2SO_4 and 0.5mol/L Na_2SO_4 solutions at the scan rate of 100mV•s-1. It is clearly seen that in the potential range -800 to 200mV, three pairs of redox peaks appeared. Mean peak potentials $E_{1/2}=(E_{pa}+E_{pc})/2$ were -638, -521 and -330mV, and peak-to-peak separations were 30, 45 and 68mV. The redox peaks correspond to one two-electron and two consecutive one-electron processes of W in compound **1**.[21]

The cyclic voltammograms of DMSO solutions of compounds **2**, **3**, **4** and **5** in the mixture of 0.5mol/L H_2SO_4 and 0.5mol/L Na_2SO_4 solutions at the scan rate of 100mV•s-1 are presented in the potential range of -800 to 200mV (Fig. s6), too. There exist three reversible redox peaks with half-wave potentials ($E_{1/2}=(E_{pa}+E_{pc})/2$) at -681, -529 and -333mV for compound **2**, half-wave potentials at -671, -532 and -290mV for compound **3**, half-wave potentials at -683, -526 and -354mV for compound **4,** and half-wave potentials at -674, -532 and -296mV for compound **5**, respectively. The redox peaks correspond to one two-electron and two consecutive one-electron processes of W in compounds **2**, **3**, **4** and **5**.[21]

Photoluminescence properties

The photoluminescence properties of DMSO solutions of compounds **1-5** were studied. The emission spectrum of compound 1 at room temperature is depicted in Fig. s7. It can be observed that an intense emission occurs at 426 nm (λex = 375 nm), which can be assigned to the emission of intra-ligand charge transfer. The emission peak in compound **1** is red shifted relative to that of the free 2,2-bpy ligand (λmax = 413nm) and that of the free inic ligand (λmax = 404nm). The red shift has been regarded as due to the complexation of the two organic ligands with the copper atom.[22] The emission spectra of compounds **2-5** at room temperature are depicted in Fig. s7. Compound **2** exhibits an emission peak at 421 nm (λex = 371 nm), compound **3** exhibits an emission peak at 399 nm (λex = 358 nm), compounds **4** and **5**, when excited at the same wavelength (370nm), show emission peaks at 415nm and 420nm, respectively. The photoluminescence mechanism of compounds **2-5** can also be attributed to the intra-ligand transition because that similar emission is also observed for pure organic ligands (Supporting Information, Fig. s7).[22]

TG analyses

The TG curve of compound **1** (Fig. s8) can be divided into three stages, the first stage is from room temperature to 252°C with a weight loss of 1.63%, which is consistent with the release of the crystallization and coordination water molecules in compound **1** (calculated: 1.45%). The second stage is from 379 to 409°C with a weight loss of 1.44%, which is due to the release of the hydroxyl ions and part of organic ligands in compound **1**. The third stage is from 409 to 656°C with a weight loss of 14.43%, which corresponds to the combustion of organic ligands in compound **1**. The total weight of the TG curve is 17.5%, which is well consistent with the calculated result 16.9%.

The TG curve of compound **3** decreases from 378 to 643°C with a weight loss of 23.64%, ascribed to the release of the organic ligands and chloride ions in compound **3** (calculated: 22.53%). Both TG curves of compounds **4** and **5** are similar to that of compound **3**, which decrease from 344 to 679°C with a weight loss of 26.27% and from 350 to 761°C with a weight loss of 22.68%, due to the combustions of the organic ligands and chloride ions in compound **4** (calculated: 25.38%) and the release of organic ligands and chloride ions in compound **5** (calculated: 22.32%), respectively.

Photodegradation properties

RhB is a typical dye contaminant that can be used for evaluating the activity of photocatalysts for the purification of waste water.[23] The performance of compounds **1-5** for photocatalytic degradation of RhB has been investigated. In a typical process, 1.0×10^{-3}mmol compound **1** (3.8mg), **2** (5.0mg), **3** (4.2mg), **4** (4.3mg) or **5** (4.1mg) was ground for about 10min with an agate mortar to obtain a fine powder, and then the powder was dispersed in 100 mL rhodamine B (RhB) solutions (1.0×10^{-5}mol·L^{-1}). The suspension was agitated in an ultrasonic bath for 20min in the dark and then magnetically stirred in the dark for about 30min. The suspension was finally exposed to irradiation from a 400W Xe lamp at a distance of about 4-5 cm between the liquid surface and the lamp. The suspension was stirred during irradiation at a stirring rate of about 790-800 rpm. At 30min intervals, 5mL of samples were taken out from the beaker, which was clarified by centrifugation at 10000 rpm for 5 min, and subsequently analyzed by UV-visible spectroscopy (Fig. 8). The photodegradation process of RhB without any photocatalyst has been studied for comparison, and only 23% of RhB was photodegraded after 360min. Changes in C_t/C_0 plot of RhB solutions versus reaction time were shown in Fig. 8. Compared with RhB without any photocatalyst, the absorption peaks of compounds **1**–**5** decreased upon irradiation, indicating that

these compounds have photocatalysis properties. It also reveals that compounds **1-5** are photocatalysts for photocatalytic degradation of RhB.

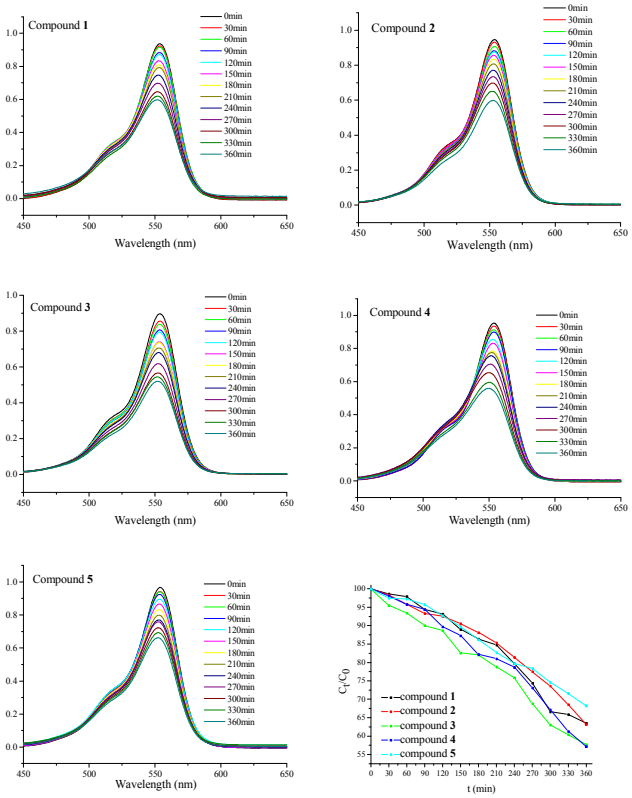

Fig. 8 photodegradation properties of compounds **1-5**.

Fig. 8 shows the reaction results of photodegradations of RhB over various catalysts at room temperature. As expected, all the catalysts are active for the photodegradation of RhB. Compound **1** catalyst shows the activity with 36.5% conversion after 360min. Nevertheless, compound **2** shows a similar activity with 36.8% conversion. Compounds **3** and **4** also show similar conversions of 42.3% and 42.8%, respectively. Compound **5** shows the lowest conversion (31.7%) of the five.

All the five compounds contain the identical Keggin ions. The photocatalytic reaction occurs in a adsorbed phase (on the surface of a catalyst), and the model of activation of catalysts is photonic activation by exciting a POM with light energy higher than the band gap of the POM, which leads to an intramolecular charge transfer and the formation of a excited-state species (POM*).[24] Therefore, POMs in catalysts are essentially important for their photodegradation properties. We think perhaps identical POMs should be the main reason why compounds **1**, **2** and compounds **3**, **4** exhibit very similar conversions.

The second main reason should be perhaps ascribed to the different packing structures of compounds **1-5**. The preferential orientations of crystal planes of compounds **1-5** should be different, thus the number of POMs on crystal planes perhaps should be different, and the difference perhaps will lead to their different photocatalytic properties. Therefore, the different photocatalytic properties of compounds **1**, **2**, compounds **3**, **4** and compound **5** can be due to the different packing structures of these compounds. Wang[25] and Wang[26] have also reported that the conversions of RhB over different compounds even containing identical Keggin species will not be the same.

Conclusions

Five new compounds based on polyoxometalates and metal mixed-organic-ligand complexes of nitrogen-containing ligands and pyridinecarboxylates have been designed and synthesized. The successful syntheses of the five compounds should be the breakthrough point for the synthesis of hybrid compounds based on mixed-organic-ligand complexes of nitrogen-containing ligands and carboxylates as well as hybrid compounds based on mixed-organic-ligand complexes of different carboxylates.

Acknowledgements

This work was supported by National Natural Science Foundation of China under Grant No. 21003056 and 51108122.

Notes and references

[a] *College of Chemistry and State Key Laboratory of Inorganic Synthesis and Preparative Chemistry, Jilin University, Changchun, Jilin, 130023. E-mail:cuixb@mail.jlu.edu.cn.*

† Footnotes should appear here. These might include comments relevant to but not central to the matter under discussion, limited experimental and spectral data, and crystallographic data.

Electronic Supplementary Information (ESI) available: [details of any supplementary information available should be included here]. See DOI: 10.1039/b000000x/

1 (a)M. T. Pope, *Heteropoly and Isopoly Oxometalates*, Springer-Verlag, Berlin, 1983; (b)M. T. Pope and A. Müller, *Angew. Chem., Int. Ed. Engl.*, 1991, **30**, 34; (c)M. T. Pope and A. Müller, *Polyoxometalates: From Platonic Solids to Anti-Retro Viral Activity*, The Netherlands, Kluwer, Dordrecht, 1994; (d)M. T. Pope and A. Müller, *Polyoxometalate Chemistry: From Topology via Self-Assembly to Applications*, the Netherlands, Kluwer, Dordrecht, 2001; (e)T. Yamase and M. T. Pope, *Polyoxometalate Chemistry for Nano-Composite Design*, the Netherlands, Kluwer, Dordrecht, 2002; (f)C. L. Hill, in *Chem. Rev.*, 1998, vol. 98; (g)D. L. Long, E. Burkholder and L. Cronin, *Chem. Soc. Rev.*, 2007, **36**, 105; (h)D. L. Long, R. Tsunashima and L. Cronin, *Angew. Chem., Int. Ed. Engl.*, 2010, **49**, 1736; (i)A. Proust, R. Thouvenot and P. Guozerh, *Chem. Commun.*, 2008, 1837; (j)A. Dolbecq, E. Dumas, C. R. Mayer and P. Mialane, *Chem. Rev.*, 2010, **110**, 6009; (k) S. Roy, *CrystEngComm*, 2014, 16, 4667.

2. (a)J. Berzelius, *Poggendorff's, Ann. Phys.*, 1826, **6**, 369; (b)J. F. Keggin, *Nature*, 1933, **131**, 908-909.
3. I. M. Mbomekalle, R. Cao, K. I. Hardcastle, C. L. Hill, M. Ammam, B. Keita, L. Nadjo and T. M. Anderson, *C. R. Chimie*, 2005, **8**, 1077-1086.
4. (a)A. Proust, B. Matt, R. Villanneau, G. Guillemot and G. L. P. Guozerh, *Chem. Soc. Rev.*, 2012, **41**, 7605; (b)J. Zhang, F. P. Xiao, J. Hao and Y. G. Wei, *Dalton Trans.*, 2012, **41**, 3599-3615; (c)P. J. Hagrman, D. Hagrman and J. Zubieta, *Angew. Chem., Int. Ed. Engl*, 1999, **38**, 2638-2684.
5. (a)X. B. Cui, J. Q. Xu, Y. Li, Y. H. Sun and G. Y. Yang, *Eur. J. Inorg. Chem.*, 2004, 1051; (b)X. B. Cui, J. Q. Xu, H. Meng, S. T. Zheng and G. Y. Yang, *Inorg. Chem.*, 2004, **43**, 8005; (c)C. L. Pan, J.

Q. Xu, G. H. Li, X. B. Cui, L. Ye and G. D. Yang, *Dalton Trans.*, 2003, 517; (d)N. Mizuno, S. Uchida, K. Kamata, R. Ishimoto, S. Nojima, K. Yonehara and Y. Sumida, *Angewandte Chemie International Edition*, 2010, **49**, 9972-9976; (e)S. Y. Shi, Y. H. Sun, Y. Chen, J. N. Xu, X. B. Cui, Y. Wang, G. W. Wang, G. D. Yang and J. Q. Xu, *Dalton Trans.*, 2010, **39**, 1389; (f)S. Y. Shi, Y. Wang, X. B. Cui, G. W. Wang, G. D. Yang and J. Q. Xu, *Dalton Trans.* , 2009, **31** 6099; (g)S. Y. Shi, Y. C. Zou, X. B. Cui, J. N. Xu, Y. Wang, G. W. Wang, G. D. Yang and J. Q. Xu, *CrstEngComm.*, 2010, **12**, 2122; (h)Y. Wang, Y. Peng, L. N. Xiao, Y. Y. Hu, L. M. Wang, Z. M. Gao, T. G. Wang, F. Q. Wu, X. B. Cui and J. Q. Xu, *CrystEngComm.*, 2012, **14**, 1049; (i)Y. Wang, L. Ye, T. G. Wang, X. B. Cui, S. Y. Shi, G. W. Wang and J. Q. Xu, *Dalton Trans.*, 2010, **39**, 1916; (j)L. N. Xiao, Y. Peng, Y. Wang, J. N. Xu, Z. M. Gao, Y. B. Liu, D. F. Zheng, X. B. Cui and J. Q. Xu, *Eur. J. Inorg. Chem.*, 2011, 1997.

6. (a) G. G. Gao, F. Y. Li, L. Xu, X. Z. Liu and Y. Y. Yang, *J. Am. Chem. Soc.*, 2008, **130**, 10838; b) H. N. Miras, E. F. Wilson and L. Cronin, *Chem. Commun.*, 2009, 1297; c) F. P. Xiao, J. Hao, J. Zhang, C. L. Lv, P. C. Yin, L. S. Wang and Y. G. Wei, *J. Am. Chem. Soc.*, 2010, **132**, 5956; d) J. Q. Sha, J. Peng, H. S. Liu, J. Chen, A. X. Tian and P. P. Zhang, *Inorg. Chem.*, 2007, **46**, 11183.
7. (a)L. Yuan, C. Qin, X. L. Wang, E. B. Wang and S. Chang, *Eur. J. Inorg. Chem.*, 2008, 4936; (b)J. Tao, X. M. Zhang, M. L. Tong and X. M. Chen, *J. Chem. Soc., Dalton Trans.*, 2001, 770; (c)C. Z. Lu, C. D. Wu, H. H. Zhuang and J. S. Huang, *Chem. Mater.*, 2002, **14**, 2649; (d)L. Lisnard, A. Dolbecq, P. Mialane, J. Marrot, E. Codjovi and F. Sécheresse, *Dalton Trans.*, 2005, 3913-3920; (e)H. Jin, Y. F. Qi, E. B. Wang, Y. G. Li, C. Qin, X. L. Wang and S. Chang, *Eur. J. Inorg. Chem.*, 2006, 4541; (f)H. Jin, Y. F. Qi, E. B. Wang, Y. G. Li, X. L. Wang, C. Qin and S. Chang, *Crystal Growth & Design.*, 2006, **6**, 2693.
8. (a)S. Reinoso, P. Vitoria, L. Lezama, A. Luque and J. M. Gutiérrez-Zorrilla, *Inorg. Chem.*, 2003, **42**, 3709; (b)S. Reinoso, P. Vitoria, L. Felices, L. Lezama and J. M. Gutiérrez-Zorrilla, *Inorg. Chem.*, 2006, **45**, 108; (c)S. Reinoso, P. Vitoria, J. M. Gutiérrez-Zorrilla, L. Lezama, L. S. Felices and J. I. Beitia, *Inorg. Chem.*, 2005, **44**, 9731; (d)X. Y. Zhao, D. D. Liang, S. X. Liu, C. Y. Sun, R. G. Gao, C. Y. Gao, Y. H. Ren and Z. M. Su, *Inorg. Chem.*, 2008, **47**, 7133-7138; (e)Y. Yang, S. X. Liu, C. C. Li, S. J. Li, G. J. Ren, F. Wei and Q. Tang, *inorg. Chem. Commun.*, 2012, **17**, 54-57; (f)Q. X. Han, P. T. Ma, J. W. Zhao, J. P. Wang and J. Y. Niu, *inorg. Chem. Commun.*, 2011, **14**, 767-770.
9. (a) C. Z. Lu, D. C. Wu, H. H. Zhuang, J. S. Huang, *Chem. Mater*., 2002, **14**, 2693; (b) S. W. Zhang, Y. X. Li, Y. Liu, R. G. Cao, C. Y. Sun, H. M. Ji, S. X. Liu, *J. Mol. Struct*., 2009, **920**, 284; (c)X. L. Wang, Q. Gao, G. C. .Liu, H. Y. Lin, A. X. Tian and J. Li, *inorg. Chem. Commun*., 2011, **14**, 745-748; (d)X. L. Wang, H. L. Hu, A. X. Tian, H. Y. Lin, J. Li and L. M. Shi, *inorg. Chem. Commun.*, 2010, **13**, 745-748; (e) Z. K. Qu, K. Yu, Z. F. Zhao, Z. H. Su, J. Q. Sha, C. M. Wang, B. B. Zhou, *Dalton Trans*., 2014, **43**, 6744.
10. L. M. Wang, Y. Wang, Y. Fan, L. N. Xiao, Y. Y. Hu, Z. M. .Gao, D. F. Zheng, X. B. Cui and J. Q. Xu, *CrstEngComm*., 2014, **16**, 430.
11. (a) Eddaoudi, M.; Moler, D. B.; Li, H. L.; Chen, B. L.; Reineke, T. M.; O'Keeffe, M.; Yaghi, O. M., *Acc. Chem. Res.* **2001,** *34*, 319-330; (b) Ockwig, N. W.; Delgado-Friedrichs, O.; O'Keeffe, M.; Yaghi, O. M., *Acc. Chem. Res.* **2005,** *38*, 176-182; (c) Phan, A.; Doonan, C. J.; Uribe-Romo, F. J.; Knobler, C. B.; O'Keeffe, M.; Yaghi, O. M., *Acc. Chem. Res.* **2010,** *43*, 58-67; (d) O'Keeffe, M.; Yaghi, O. M., *Chem. Rev.* **2012,** *112*, 657-702; (e) Long, J. R.; Yaghi, O. M., *Chem. Soc. Rev.* **2009,** *38*, 1213; (f) Férey, G., *Chem. Soc. Rev.* **2008,** *37*, 191.
12. (a)A. Dolbecq, P. Mialane, L. Lisnard, J. Marrot and F. Sécheresse, *Chem. Eur. J.*, 2003, **9**, 2914; (b)P. Mialane, A. Dolbecq and F. Sécheresse, *Chem. Commun.*, 2006, 3477; (c)S. T. Zheng, J. Zhang and G. Y. Yang, *Angew. Chem. Int. Ed.*, 2008, **47**, 3909; (d)G. Rousseau, O. Oms, A. Dolbecq, J. r. m. Marrot and P. Mialane, *Inorg. Chem.*, 2011, **50**, 7376-7378; (e)B. Nohra, H. El Moll, L. M. Rodriguez Albelo, P. Mialane, J. r. m. Marrot, C. Mellot-Draznieks, M. O'Keeffe, R. Ngo Biboum, J. l. Lemaire, B. Keita, L. Nadjo and A. Dolbecq, *J. Am. Chem. Soc.*, 2011, **133**, 13363-13374.
13. a) H. D. Yin, C. H. Wang, Y. Wang, C. L. Ma and G. F. Liu, *Youji Huaxue.*, 2002, **22**, 575; b) Y. H. Liu, Y. L. Lu, H. L. Tsai, J. C. Wang and K. L. Lu, *J. Solid. State. Chem.*, 2001, **158**, 315; c) C. Z.-J. Lin, S. S.-Y. Chui, S. M.-F. Lo, F. L.-Y. Shek, M. M. Wu, K. Suwinska, J. Lipkowski and I. D. Williams, *Chem. Commun.*, 2002, 1642; d) J. Y. Kim, A. J. Norquist and D. O'hare, *Chem. Mater.*, 2003, **15**, 1970; e) D. Hshizume and Y. Ohashi, *J. Chem. Soc., Perkin Trans.*, 1998, **2**, 1931; f) H. Y. An, Y. G. Li, E. B. Wang, D. R. Xiao, C. Y. Sun and L. Xu, *Inorg. Chem.*, 2005, **44**, 6062; g) S. Gao, Z. B. Zhu, L. H. Huo and H. Zhao, *Acta Crystallogr., Sec. E.*, 2005, **61**, m656.
14. X. M. Zhang, *Coord. Chem. Rev*, 2005, **249**, 1201-1219.
15. a) S. Chattopadhyay, P. E. Fanwich and R. A. Walton, *Inorg. Chim. Acta.*, 2004, **357**, 764; b) T. Brasey, R. Scopelliti and K. Severin, *Inorg. Chem.*, 2005, **44**, 160; c) P. C. R. Soares-santos, H. I. S. Nogueira, J. Rocha, V. Felix, M. G. B. Drew, R. A. S. Ferreira, L. D. Carlos and T. Trindade, *Polyhedron.*, 2003, **22**, 3529; d) S. M. O. Quintal, H. I. S. Nogueira, V. Felix and M. G. B. Drew, *Polyhedron.*, 2002, **21**, 2783.
16. a) H. D. Yin, C. H. Wang, C. L. Ma, Y. Wang and H. X. Fang, *Chinese J. Struct. Chem.*, 2003, **22**, 211; b) W. Chen, H. M. Yuan, J. Y. Wang, Z. Y. Liu, J. J. Xu, M. Wang and J. S. Chen, *J. Am. Chem. Soc.*, 2003, **125**, 9266; c) W. B. Lin and P. Ayyappan, *Polyhedron.*, 2003, **22**, 3037; d) D. F. Mullica, E. L. Sappenfield and J. E. Bradshaw, *Powder Diffraction.*, 1986, **1**, 261; e) R. Song, K. M. Kim and Y. S. Sohn, *Inorg. Chim. Acta.*, 2000, **304**, 156; f) M. Toma, A. Sanchez, J. S. Casas, J. Sordo, M. S. Garcia-Tasende, E. E. Castellano, J. Ellena and I. Berdan, *U. S. Army, Tech. Report.*, 2003, **4**, 441; g) W. T. Chen, L. Hu, C. Q. Lai and W. J. Zhou, *J. Chem. Res.*, 2010, **34**, 533; h) W. J. Feng, G. P. Zhou, X. F. Zheng, Y. G. Liu and Y. Xu, *Acta Crystallogr., Sec. E.*, 2006, **62**, m2033.
17. a) A. Mangia, M. Nardelli, C. Pelizzi and G. Pelizzi, *J. Chem. Soc., Dalton Trans.*, 1972, 2483; b) D. G. Huang, W. G. Wang, X. F. Zhang, C. N. Chen, F. CHen, Q. T. Liu, D. Z. Liao, L. C. Li and L. C. Sun, *Eur. J. Inorg. Chem.*, 2004, 1454; c) P. G. Harrison and R. C. Philips, *J. Organomet. Chem.*, 1979, **182**, 37.
18. I. D. Brown, in *Structure and Bonding in Crystals*, eds. M. O'Keefe and A. Navrotsky, Academic Press, New York, 1981, pp. 1–30.
19. C. Rocchiccioli-deltcheff, M. Fournier and R. Franck, *Inorg. Chem.*, 1983, **22**, 207-216.
20. J. Ghijsen, L. H. Tjeng, J. v. Elp, H. Eskes, J. Westerink and G. A. Sawatzky, *Phys. Rev. B*, 1988, **38**, 11322-11330.

21. a) S. Q. Liu, Z. Shi and S. J. Dong, *Electroanalysis*, 1998, **10**, 891-896; b) A. X. Tian, J. Ying, J. Peng, J. Q. Sha, H. J. Pang, P. P. Zhang, Y. Chen, M. Zhu and Z. M. Su, *Inorg. Chem.*, 2009, **48**, 100.
22. a) J. R. Lakowicz, *Principles of Fluorescence Spectroscopy*, Springer, Berlin, 2006; b) B. Valeur, *Molecular Fluorescence: Principles and Application*, Wiley-VCH, Weinheim, 2002.
23. a) J. Lü, J. X. Lin, X. L. Zhao and R. Cao, *Chem. Commun*., 2012, **48**, 669; b) J. Q. Sha, J. W. Sun, M. T. Li, C. Wang, G. M. Li, P. F. Yan and L. J. Sun, *Dalton Trans*., 2013, **42**, 1667.
24. a) H. Fu, Y. G. Li, Y. Lu, W. L. Chen, Q. Wu, J. X. Meng, X. L. Wang, Z. M. Zhang and E. B. Wang, *Cryst. Growth Des.*, 2011, **11**, 458; b) D. Y. Chen, A. Sahasrabudhe, P. Wang, A. Dasgupta, R. X. Yuan, S. Roy, *Dalton Trans.*, 2013, **42**, 10587.
25. Q. Lan, J. Zhang, Z. M. Zhang, Y. Lu and E. B. Wang, *Dalton Trans.*, 2013, **42**, 16602.
26. a) X. L. Wang, D. Zhao, A. X. Tian and J. Ying, *Dalton Trans.*, 2014, **43**, 5211; b) X. L. Wang, N. Han, H. Y. Lin, A. X. Tian, G. C. Liu and J. W. Zhang, *Dalton Trans.*, 2014, **43**, 2052.

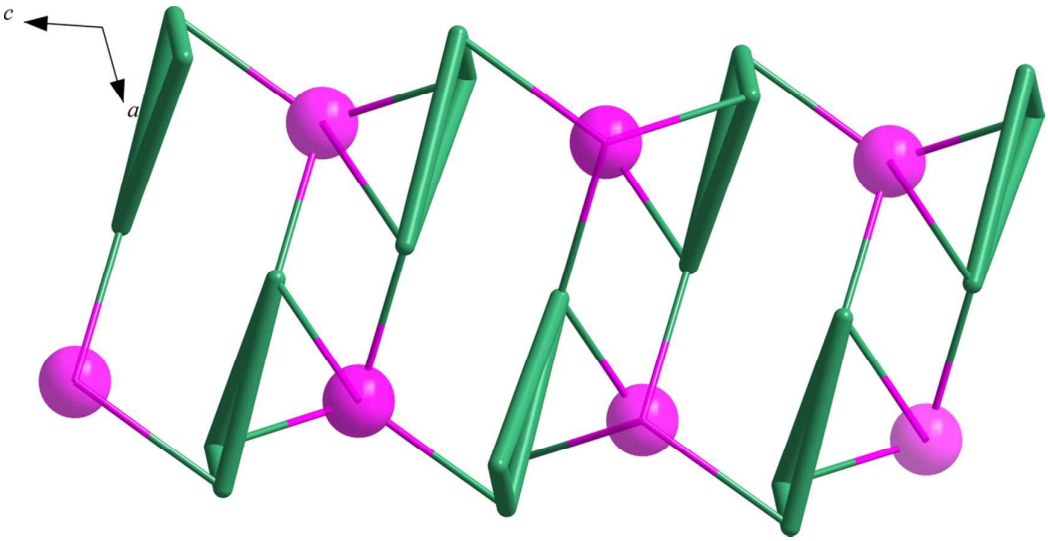

Five compounds exhibiting novel structures constructed from polyoxoanions and metal mixed-organic complexes of carboxylates and nitrogen-containing ligands have already been synthesized and characterized.